Unimolecular Reactions of Proton-Bound Cluster Ions: Competition between Dissociation and Isomerization in the Methanol−Acetonitrile Dimer

Paul M. Mayer

Department of Chemistry, University of Ottawa, Ottawa, Canada K1N 6N5

Received: November 18, 1998; In Final Form: February 11, 1999

The metastable proton-bound dimer of acetonitrile and methanol, $(CH_3CN)(CH_3OH)H^+$, exhibits two unimolecular reactions on the microsecond time scale, a simple bond cleavage reaction to form CH_3CNH^+ and CH_3OH, and the loss of water to form $CH_3CNCH_3^+$. The latter process is preceded by the isomerization of the proton-bound dimer to a second isomer, $(CH_3CNCH_3)(H_2O)^+$. Collision-induced dissociation mass spectrometry was used to identify the two sets of reaction products, and the results of isotopic labeling experiments suggest that there is a rate-limiting isomerization step going from the proton-bound dimer to the second complex. The competition between the two channels was modeled with ab initio calculations and RRKM rate theory to obtain relative energies for the reaction surface. The transition structure for the rate-determining isomerization could not be located with ab initio calculations, and so its relative energy was estimated using RRKM theory. The 0 K binding energy of the $(CH_3CN)(CH_3OH)H^+$ complex was calculated to be 121 kJ mol^{-1} at the G2 level of theory (relative to the dissociation products CH_3CNH^+ and CH_3OH).

1. Introduction

The study of clusters of organic and inorganic molecules has seen a dramatic growth over the past 20 years. Clusters of molecules can be viewed as an intermediate state of matter between the dilute gas phase and solution, and studying them allows the effects of solvation on the chemistry of gas-phase molecules and ions to be explored.[1] Ionic clusters (typically made up of a core ion surrounded by one or more solvating molecules) are known to be involved in the chemistry of the upper and mid-atmosphere.[2]

A central issue when studying the chemistry of gaseous ions is their propensity for rearrangement prior to reaction. Over the years, a variety of thermodynamically stable structures have been discovered that have key roles in ion dissociation mechanisms, including distonic ions,[3] ion−neutral complexes,[4] and bridged ions.[5] The isomerization of more conventional organic ions is well-known and appears to be a common occurrence.[6] However, the isomerization reactions of cluster ions have not been extensively studied.[7]

The family of proton-bound mixed dimers consisting of nitriles and alcohols all have at least one common feature; they all exhibit the competition between simple-bond dissociations and dehydration reactions in their metastable ion mass spectra. In this respect they are similar to many proton-bound alcohol dimers.[7c,8] The dehydration of these simple clusters necessarily involves the isomerization of the proton-bound entity to an isomeric form. Previous studies on these and related systems have focused on the distribution of cluster sizes formed in molecular beam experiments and on the enthalpies of successive addition of neutral monomers to proton-bound clusters of acetonitrile with water and methanol.[9]

The present study looks at the unimolecular chemistry of one of the first members in this series of nitrile−alcohol clusters, the proton-bound dimer of acetonitrile and methanol. The goals are to identify with mass spectrometry and ab initio theory the key features of the potential energy surface that play a role in the chemistry of these dimer ions.

2. Experimental Procedures

All experiments were performed on a modified VG ZAB-2HF mass spectrometer, incorporating a magnetic sector followed by two electrostatic sectors (BEE geometry).[10] Cluster ions were generated by self-protonation and subsequent ion−molecule reaction in the ion source of the ZAB with the CI slit in place. The pressure in the source chamber, read with an ion gauge located above the ion source diffusion pump, was typically between 10^{-5} and 10^{-4} Torr. Below 10^{-5} Torr, no cluster ions were generated, and there was no evidence of clusters larger than the dimers at any of the source pressures in this study. Metastable ion (MI) and collision-induced dissociation (CID) mass spectra were recorded in the typical fashion.[11] Helium collision gas was used in all CID experiments (spectra were obtained under single-collision conditions, i.e., 10% beam reduction).

Acetonitrile and methanol were obtained from commercial sources and used without further purification. Labeled compounds were obtained from MSD Isotopes.

3. Computational Procedures

Standard ab initio molecular orbital calculations[12] were performed using the GAUSSIAN 94[13] suite of programs. Geometry optimizations were carried out at the HF/6-31G(d), MP2/6-31G(d), and MP2/6-31+G(d) levels of theory. A recent assessment of theoretical procedures for describing proton-bound dimers involving HCN and CH_3CN with a variety of first-row hydrides has shown that geometries optimized at the MP2/6-31+G(d) level of theory provide an adequate foundation for high-level single-point energy calculations.[14] Vibrational frequencies were calculated at the HF/6-31G(d) and MP2/6-31G(d) levels of theory. Transition states were confirmed by the intrinsic reaction coordinate procedure in GAUSSIAN 94.

Single-point energies on the MP2/6-31+G(d) geometries were obtained at the G2,[15] G2(MP2),[16] G2(MP2,SVP),[17] and G2(ZPE=MP2)[18] levels of theory. Scaling factors for zero-point energies (ZPE) used in these high-level treatments were those

10.1021/jp984473s CCC: $18.00
Published on Web 04/22/1999

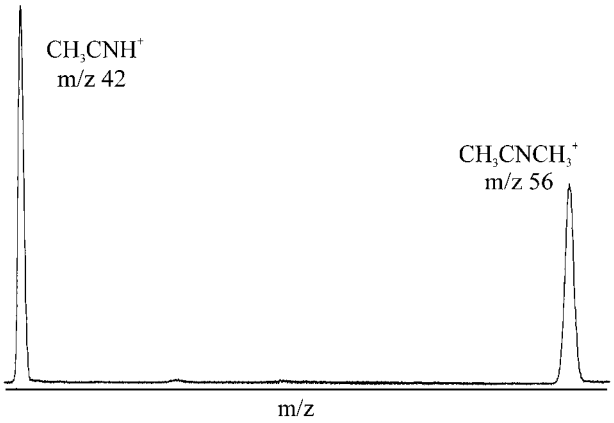

Figure 1. MI mass spectrum of $(CH_3CN)(CH_3OH)H^+$ obtained in the second field-free region of the ZAB-2HF.

TABLE 1: Relative Peak Intensities in the Mass Spectra of $(CH_3CN)(CH_3OH)H^+$

precursor	$CH_3CNH^+ + CH_3OH$	$CH_3CNCH_3^+ + H_2O$
MI Mass Spectrum[a]		
$(CH_3CN)(CH_3OH)H^+$, *m/z* 74	1.0 (42)	0.57 (56)
$(CH_3CN)(CH_3OH)H^+$, *m/z* 74	1.0 (42)[b]	1.0 (56)[b]
$(CD_3CN)(CH_3OH)H^+$, *m/z* 77	1.0 (45)	0.3 (59)
$(CH_3CN)(CD_3OH)H^+$, *m/z* 77	1.0 (42)	0.3 (59)
$(CH_3CN)(CD_3OD)H^+$, *m/z* 78	1.0 (42), 0.43 (43)	0.3 (59)
$(CH_3CN)(CD_3OD)D^+$, *m/z* 79	1.0 (43)	0.23 (59)
CID Mass Spectrum[a]		
$(CH_3CN)(CH_3OH)H^+$, *m/z* 74	1	0.23

[a] Observations in the 2FFR of the instrument unless otherwise stated. Product ion *m/z* ratio in parentheses. [b] 3FFR observation.

recommended for the individual procedures (i.e., HF/6-31G(d) ZPEs scaled by 0.8929 for G2, G2(MP2), and G2(MP2,SVP), and MP2/6-31G(d) ZPEs scaled by 0.9646 for G2(ZPE=MP2)). The geometric and energetic changes in going from MP2(full)/6-31G(d) to MP2/6-31G(d), which employs a frozen core, were found to be minor.

Thermal corrections to the data were uniformly carried out using the HF/6-31G(d) vibrational frequencies (scaled by 0.8929). Experimental $\Delta_f H°$ data reported only at 298 K were converted to 0 K values using the above theoretical corrections. Theoretical heats of formation at 0 K were derived by the atomization method,[19] together with experimental heats of formation of the constituent atoms.[20]

4. Results and Discussion

Mass Spectrometry. *Metastable $(CH_3CN)(CH_3OH)H^+$ Ions*. The MI mass spectrum (Figure 1) of the mixed proton-bound dimers of acetonitrile and methanol, $(CH_3CN)(CH_3OH)H^+$, *m/z* 74, exhibits two peaks, one due to *m/z* 42 (−32 amu) and the other due to *m/z* 56 (−18 amu), which are nominally due to the loss of methanol and water, respectively.

The relative intensities of the two peaks change in going from the second field-free region (2FFR) to the 3FFR of the instrument (Table 1). The greater relative abundance of *m/z* 56 at longer lifetimes indicates that this process has the tighter transition state. Upon admission of a trace amount of collision gas into a collision cell (2FFR pressure reading of 3×10^{-8} Torr), the peak with *m/z* 42 exhibits a substantial increase in intensity, while the peak with *m/z* 56 is largely unaffected. This is an indication that the latter channel is due to the dissociation of an isomeric form of the original proton-bound dimer and is consistent with there being a tight transition state in the reaction. In addition, it suggests that the key rate-limiting step in the water loss channel is the initial isomerization reaction out of the potential well containing the proton-bound dimer. There is insufficient isomer present in the mass-selected ion beam for them to contribute to the CID mass spectrum (at very low target pressures). The kinetic energy release (KER) values for the two processes (reported from the full-width at half-height of the two peaks, $T_{0.5}$) are 6 meV (*m/z* 42) and 19 meV (*m/z* 56). The 6 meV value is indicative of a true threshold process, while the 19 meV $T_{0.5}$ is consistent with the dissociation of a weakly bound species (more will be said on this point later).

Identity of the Fragment Ions. The two metastably generated fragment ions, *m/z* 42 and *m/z* 56, were each transmitted into the 3FFR of the apparatus and their respective He CID mass spectra obtained. Ions with *m/z* 42 were identified as protonated acetonitrile, the He CID mass spectrum being identical to that obtained for *m/z* 42 ions generated in the ion source when only CH_3CN was present. This is consistent with the loss of 32 amu in the form of a neutral methanol molecule. The He CID mass spectrum of the metastably generated *m/z* 56 ions was found to be most similar to that of $CH_3CNCH_3^+$ (generated by the association reaction of CH_3^+ with CH_3CN).[21] This channel, which produces neutral water, obviously involves the rearrangement of the originally formed proton-bound dimer into at least one isomer.

Isotopic Labeling Studies. To identify possible products of isomerization reactions, deuterium-labeled cluster ions were generated in the ion source. The cluster ions $(CD_3CN)(CH_3OH)H^+$ (*m/z* 77, formed by the reaction of CD_3CN with CH_3OH) exhibit only two fragment ion peaks in their MI mass spectrum (Table 1), *m/z* 45 (CD_3CNH^+) and *m/z* 59 ($CD_3CNCH_3^+$), the identity of these ions being confirmed by their CID mass spectra.[22] These results show that no reversible exchange takes place between the methyl hydrogens on acetonitrile and the other hydrogens, the labels being retained 100% by acetonitrile.

The reaction of perdeuterated methanol, CD_3OD, with CH_3CN in the ion source of the instrument results in three labeled cluster ions: *m/z* 77, $(CH_3CN)(CD_3OH)H^+$, *m/z* 78 $(CH_3CN)(CD_3OD)H^+$, and *m/z* 79 $(CH_3CN)(CD_3OD)D^+$, although the location of the label among the bridging hydrogens of *m/z* 78 cannot be determined (the bridging hydrogens are defined here as the bridging proton and the hydroxy hydrogen on methanol). The loss of label in *m/z* 77 and *m/z* 78 is the result of exchange that takes place between the labile hydroxy hydrogen on methanol and the walls of the sample inlet system of the instrument. The MI mass spectra of all three clusters are consistent with the results obtained for the cluster with CD_3CN, i.e., no significant exchange takes place between the hydrogens on the terminal methyl groups of the cluster and the bridging hydrogens. The cluster with *m/z* 77 yields only CH_3CNH^+ (*m/z* 42) and $CH_3CNCD_3^+$ (*m/z* 59, loss of H_2O). The cluster with *m/z* 78 yields both CH_3CNH^+ and CH_3CND^+ along with $CH_3CNCD_3^+$ (loss of HOD). There is also a very small but real peak at *m/z* 60 (~2% of *m/z* 59) that is not totally removed by subtracting the ^{13}C contribution from *m/z* 77. This nonzero signal suggests that a small percentage of these cluster ions may be formed with deuterium already incorporated in the acetonitrile methyl group ($(CH_2DCN)(CD_3OH)H^+$). It is not the result of exchange in the cluster ions, however, since there is no evidence of such a reaction for *m/z* 77. A similar situation arises for *m/z* 79, which yields primarily CH_3CND^+ and $CH_3CNCD_3^+$ (loss of D_2O). The 2:1 ratio for formation of CH_3CNH^+ and CH_3CND^+ from *m/z* 78 suggests an isotope effect favoring the proton remaining with the departing CH_3CN group.

TABLE 2: Comparison of Experimental and Calculated 298 K Heats of Formation

	$\Delta_f H°_{298}$ [a]				
species	G2	G2(MP2)	G2(MP2,SVP)	G2(ZPE=MP2)	exptl[b]
I	497.9	495.1	495.4	492.2	
II	480	476.4	473.7	477	
III	487.8	484.3	481.6	484.4	
$CH_3CNCH_3^+$	763.8	763.4	756.9	761.1	786[c]
CH_3CNH^+	826.9	826.7	821.6	823.5	817 (825[d])
CH_3OH	−207	−209.4	−205.6	−207.5	−201.6 ± 0.2
H_2O	−243	−246.1	−242.2	−243.8	−241.83

[a] In kJ mol^{-1}. [b] Lias et al.[20] unless otherwise stated. [c] Smith et al.[21b] [d] On the basis of the PA value of CH_3CN quoted by Hunter and Lias.[23]

From Table 1, it is seen that when deuterium is in the bridge, isomerization competes less effectively with the simple dissociation. The relative abundance of simple cleavage and isomerization changes from 1:0.3 when H is in the bridge to ca. 1:0.22 with D in the bridge (a factor of 1.5).

Reaction Mechanism. The dissociation of metastable ions $(CH_3CN)(CH_3OH)H^+$ into $CH_3CNH^+ + CH_3OH$ and $CH_3CNCH_3^+ + H_2O$ involves the competition between a bond-cleavage reaction and an isomerization reaction. In addition, from the experiments involving the introduction of a trace amount of collision gas, it can be concluded that the key competition is between cleavage and isomerization of the originally formed proton-bound dimer. The results of the labeling experiments are consistent with a model for the reaction that involves one key, thermodynamically stable isomer (or a limited number of stable isomers) but not one that incorporates a large number of isomeric complexes having small barriers of interconversion (that can interconvert rapidly prior to dissociation). Such mechanisms tend to result in the loss of positional identity of isotopic labels. The heats of formation of the products are known (Table 2), but the binding energy of the proton-bound dimer is not, nor is the height of the isomerization barrier or the binding energy of the key isomer on the surface. However, the competition between the bond cleavage and isomerization suggests that the barrier leading to the isomer is probably comparable in energy to the $CH_3CNH^+ + CH_3OH$ product channel energy.

The water loss products lie 90 kJ mol^{-1} below $CH_3CNH^+ + CH_3OH$ (Table 2) and so will be formed with considerable excess energy. The small $T_{0.5}$ value (19 meV) for the dehydration channel indicates that only a small fraction of this excess energy is partitioned among the translational degrees of freedom of the products, suggesting an early transition state that resembles the proton-bound dimer. Such a result is consistent with a dissociation involving the formation of an intermediate, weakly bound species and has been observed previously for the dissociation of $^{\bullet}CH_2CH_2OH_2^+$ ions (which isomerize to the [ethene−water]$^{\bullet+}$ ion−molecule complex prior to dehydration).[24]

The surface was further explored using ab initio calculations, which are discussed below.

Ab Initio Calculations. *Identifying Isomers of the Proton-Bound Dimer.* The mass spectrometric results presented above indicate that there is likely a key, thermodynamically stable isomer in the reaction that is responsible for water loss. We have used ab initio calculations to identify this isomer and model the reaction surface.

Only two stable isomers were located, **II** and **III**. The structures of the proton-bound dimer (**I**) and isomers **II** and **III** and $CH_3CNCH_3^+$ are shown in Figure 2. Isomers **II** and **III** are ion−molecule complexes between $CH_3CNCH_3^+$ and water. In **II**, the water is complexed near the CN group of the *m*/*z* 56 ion, while in **III** it is complexed to the terminal methyl group

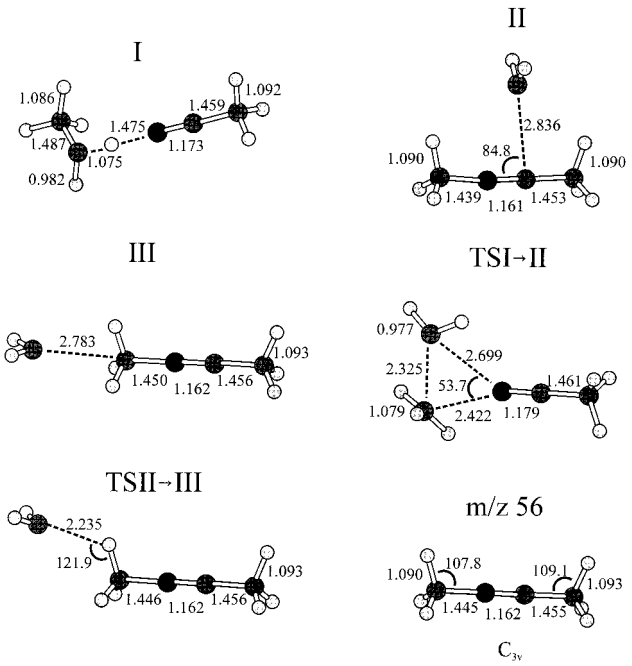

Figure 2. Partial geometries for the proton-bound dimer **I** and isomers **II** and **III**, transition structures for their interconversion (**TSI → II** and **TSII → III**), and the fragment ion *m*/*z* 56. While **TSI → II** was found to connect isomers **I** and **II**, its high relative energy (Table 3) probably means that it is not involved in the interconversion in the present experiment (see text). All geometries are optimized at the MP2/6-31+G(d) level of theory. Bond lengths are in angstroms and bond angles in degrees.

opposite the nitrogen. Other structures involving moving the water to other locations are all optimized to either **II** or **III**. Structures having two hydroxy hydrogens H-bonded to the acetonitrile or to complexes between CH_3CNH^+ and methanol (not bound through a hydrogen bond to oxygen) all optimized to the original proton-bound dimer. The relative energies of these three isomers at the HF and MP2 levels of theory indicated that both **II** and **III** were thermochemically more stable than the proton-bound dimer, with **II** being slightly lower in energy than **III**. Transition structures connecting the proton-bound dimer to **II** (**TSI → II**) and connecting **II** to **III** (**TSII → III**) were found and are also shown in Figure 2.

Relative Energies. Calculated heats of formation of equilibrium species are listed in Table 2 and relative energies in Table 3. Two features are apparent from Table 3. The first is that the barrier to interconversion of isomers **II** and **III** (**TSII → III**) is trivial (8.6 kJ mol^{-1} in the forward direction), and at the internal energies probed in our experiments, the water most likely migrates freely around the $CH_3CNCH_3^+$ moiety. The second is the energy of the transition structure connecting the proton-bound dimer and **II** (**TSI → II**). The G2 energy of **TSI → II** (which was confirmed by IRC in GAUSSIAN 94) is 110 kJ

TABLE 3: Comparison of the 0 K Relative Energies (in kJ mol^{-1}) Calculated at a Variety of Levels of Theory

	HF/ 6-31G(d)[a]	MP2/ 6-31G(d)[a]	MP2/ 6-31+G(d)[a]	G2[a]	G2 (MP2)[a]	G2 (MP2,SVP)[a]	G2 (ZPE=MP2)
I	0	0	0	0	0	0	0
II	−22.2	−11.3	−23.4	−20.7	−21.5	−24.5	−18
III	−13.9	−1.3	−13.8	−13.7	−14.4	−17.5	−11.5
TSI−II	188.3	241.7	228.4	230.8	231	229.5	236.3
TSII−III	−12.3	−0.2	−12.6	−12.1	−12.7	−15.7	−9.9
$CH_3CNH^+ + CH_3OH$	109.2	137.8	129	121	121	119.4	122.7
$CH_3CNCH_3^+ + H_2O$	20.4	39.4	24.4	18.6	17.6	14.7	20.4

[a] HF/6-31G(d) ZPE (scaled by 0.8929).

TABLE 4: Summary of G2 Data for Relative Energies and Heats of Formation

	relative energy (kJ mol^{-1})		$\Delta_f H°$ (kJ mol^{-1})	
	0 K	298 K	0 K	298 K
I	0	0	522	498
II	−21	−18	501	480
III	−14	−10	508	488
TSI → II	231 (115)[a]	237 (121)[a]		
TSII → III	−12	−10		
$CH_3CNH^+ + CH_3OH$	121	122	643	620
$CH_3CNCH_3^+ + H_2O$	19	23	540	521

[a] Results of RRKM modeling.

mol^{-1} above the dissociation products $CH_3CNH^+ + CH_3OH$ (Table 3). It will become clear below that this is far too high for it to be significant in the unimolecular reactions of **I** under the present experimental conditions. Either the energy is poorly defined with G2 theory or, more likely, there is an alternative transition structure (or series of transition structures) leading from the proton-bound dimer to the well containing **II** and **III**. We have been unable to locate such a transition structure, but this does not preclude its existence.

A variety of levels of theory were employed to determine the relative energies and thus assess their performance relative to standard G2 theory. The three G2 methods G2, G2(MP2), and G2(MP2,SVP) all give comparable relative energies, with G2(MP2) deviating from G2 theory by less than 1 kJ mol^{-1} and G2(MP2,SVP) deviating by less than 3.1 kJ mol^{-1} (Table 3). G2(ZPE=MP2) deviates significantly more, up to 6.8 kJ mol^{-1} in the case of **TSI → II**. This is principally due to the difference in ZPE calculated for these species at the HF/6-31G(d) and MP2/6-31G(d) levels of theory. The direct methods (HF/6-31G(d), MP2/6-31G(d), and MP2/6-31+G(d)) all give results in qualitative agreement with the composite methods. The best agreement is for MP2/6-31+G(d), which provides relative energies that are fairly close to the G2 results (maximum deviation of 8 kJ mol^{-1}).

The relative energies and heats of formation at 0 and 298 K obtained at the G2 level of theory are summarized in Table 4. The 0 K binding energy of the proton-bound dimer (relative to dissociation) is 121 kJ mol^{-1} at the G2 level of theory, yielding a $\Delta_f H°_0$ of 522 kJ mol^{-1} (498 kJ mol^{-1} at 298 K). El-Shall et al.[9b] have made equilibrium measurements for proton-bound clusters containing acetonitrile and methanol. Our calculated binding energy of the dimer is consistent with their results, which are for the addition of CH_3CN and/or CH_3OH to the dimer (they were unable to determine the binding energy of the dimer itself). The enthalpy they determined for the addition of CH_3OH to $(CH_3CN)(CH_3OH)H^+$ was 87.4 kJ mol^{-1}, while that for the addition of CH_3CN was 94.6 kJ mol^{-1}. As substrate molecules are added, their binding energies will decrease, and the present results are indicative of that. In addition, our calculated $\Delta_f H°$ for the proton-bound dimer fixes the absolute heats of formation of all of the clusters in their study (Table 5).

TABLE 5: Heats of Formation for Proton-Bound Clusters of Methanol with Acetonitrile[a]

cluster	$\Delta_f H°_0$ (kJ mol^{-1})	$\Delta_f H°_{298}$ (kJ mol^{-1})
$(CH_3CN)(CH_3OH)H^+$	522[b]	498[b]
$(CH_3CN)_2(CH_3OH)H^+$	509	477
$(CH_3CN)_3(CH_3OH)H^+$	560	522
$(CH_3CN)(CH_3OH)_2H^+$	245	209
$(CH_3CN)(CH_3OH)_3H^+$	42	−6.5
$(CH_3CN)_2(CH_3OH)_2H^+$	262	218

[a] Estimated using the present result for the proton-bound dimer and the relative enthalpies derived by El-Shall et al.[9b] [b] This work.

The binding energy of **II** is quite small, 40 kJ mol^{-1}, which is consistent with there being a relatively small population of these ions in the beam flux at any given time. The small binding energy is also consistent with the fact that it is not a proton-bound complex but rather an ion−molecule complex in which the charge is delocalized over the four heavy atoms in the $CH_3CNCH_3^+$ moiety (Mulliken population analysis for the optimized structure has each carbon with ∼0.5 of a positive charge, the nitrogen being partially negative). The above value of 40 kJ mol^{-1} is similar to that for other non-hydrogen-bonded ion−molecule complexes in which the charge may be diffusely spread over one partner (Daly et al.[25] have determined the binding enthalpy of [benzene−acetonitrile]$^{\bullet+}$, 57 kJ mol^{-1}, and estimated the binding enthalpy of [benzene−methanol]$^{\bullet+}$ to be 48 kJ mol^{-1}). The presence of isomer **II** is consistent with the small value for the KER observed for the water loss reaction (see above).

Kinetic Modeling. The reactions can be kinetically modeled with RRKM theory[26] to determine the relative energy of the barrier leading from **I** to **II**. The microcanonical rate constant, $k(E)$, is a function of the density (ρ) and sum ($N^{\ddagger}$) of states of the reacting ion and transition state, respectively. In its simplest form,

$$k(E) = \frac{\sigma}{h}\frac{N^{\ddagger}(E-E_0)}{\rho(E)}$$

where E represents the internal energy of the reacting ion, E_0 is the 0 K activation energy, σ is the symmetry number, and h is Planck's constant. In the present study, the sums and densities of states were calculated using the Beyer−Swinehart direct-count algorithm[26] employing scaled MP2/6-31G(d) harmonic vibrational frequencies (Table 6) and the rate constants were calculated employing the G2 0 K activation energies (Table 4).

There are four elementary reactions that need to be addressed, two dissociation reactions and the forward and reverse isomerization reactions (the interconversion of **II** and **III** will be so fast that the second potential well was approximated using only isomer **II**). For the reaction leading from the proton-bound dimer

TABLE 6: Vibrational Frequencies Used in the RRKM Analysis

species	harmonic vibrational frequencies (cm^{-1})[a]
I	1, 66, 81, 127, 147, 263, 345, 349, 508, 891, 915, 958, 1024, 1024, 1083, 1155, 1279, 1380, 1424, 1430, 1430, 1459, 1461, 1647, 1908, 2170, 2950, 2986, 3047, 3047, 3105, 3121, 3487
II	50, 87, 99, 139, 180, 194, 223, 265, 330, 357, 358, 679, 1010, 1024, 1064, 1107, 1116, 1362, 1402, 1416, 1426, 1440, 1443, 1649, 2290, 2945, 2965, 3044, 3049, 3078, 3079, 3543, 3656
TS for **I** → **II/III**	(−508), 1, 66, 81, 127, 147, 263, 345, 349, 891, 915, 958, 1024, 1024, 1083, 1155, 1279, 1380, 1424, 1430, 1430, 1459, 1461, 1647, 1908, 2170, 2950, 2986, 3047, 3047, 3105, 3121, 3487
TSI → products	(−263),[b] 1, 40, 49, 77, 89, 207, 210, 508, 891, 915, 958, 1024, 1024, 1083, 1155, 1279, 1380, 1424, 1430, 1430, 1459, 1461, 1647, 1908, 2170, 2950, 2986, 3047, 3047, 3105, 3121, 3487
TSII → products	(−139),[b] 28, 49, 55, 77, 100, 135, 265, 330, 357, 358, 679, 1010, 1024, 1064, 1107, 1116, 1362, 1402, 1416, 1426, 1440, 1443, 1649, 2290, 2945, 2965, 3044, 3049, 3078, 3079, 3543, 3656

[a] MP2/6-31G(d) frequencies, scaled by 0.9434 as recommended by Scott and Radom.[26] [b] Corresponds to the vibrational mode in **I** or **II** that most closely matches the dissociation reaction.

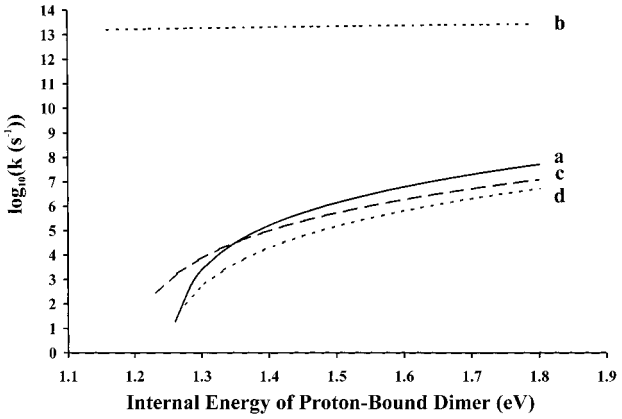

Figure 3. Plot of log $k(E)$ vs ion internal energy curves for the three principle reactions of $(CH_3CN)(CH_3OH)H^+$ (all energies are referenced to the ground state of the proton-bound dimer): (a) the dissociation of **I** into CH_3CNH^+ and CH_3OH; (b) the dissociation of **II** into $CH_3CNCH_3^+$ and H_2O; (c) the forward isomerization reaction of **I** to **II** using an E_0 of 115 kJ mol^{-1}; (d) the forward isomerization reaction of **I** to **II** using an E_0 of 125 kJ mol^{-1}.

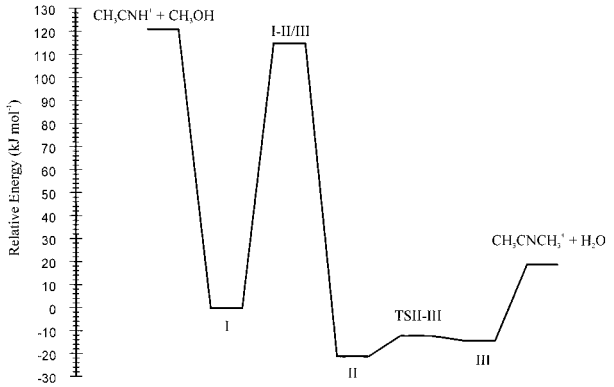

Figure 4. Theoretical reaction profile for $(CH_3CN)(CH_3OH)H^+$. All energies are G2 values except for the barrier to isomerization from **I** to **II/III** (**I** → **II/III**), which was obtained from the kinetic modeling of the forward isomerization reaction (see text). All values are in kJ mol^{-1}.

to products, the vibration corresponding to the almost free internal rotation about the proton bridge (1 cm^{-1}) was not included in the $\rho(E)$ and $N^{\ddagger}(E-E_0)$ calculations as a distinct vibration; rather, it was included as a hindered internal rotor with a rotational constant of 23.8 GHz. For each dissociation reaction, the transition-state frequencies were estimated by using the frequencies calculated for **I** and **II**, respectively, removing one in each case that corresponded to stretching of the necessary bond and scaling the lowest five frequencies to obtain an entropy of activation, $\Delta S^{\ddagger}(600\ K)$, of approximately 12 J K^{-1} mol^{-1}. This latter value is not untypical for simple bond cleavage reactions.[26] The results are plotted in Figure 3. Clearly, the loss of water from **II** is fast enough to preclude the reverse isomerization to **I** from being a significant process. This is consistent with the experimental result that no isotopic scrambling occurs in the labeled clusters.

It is apparent from the relative energy of **TSI** → **II** that it is not involved in the reaction. Thus, the forward isomerization of **I** to the well containing **II**/**III** was modeled using transition-state frequencies that were estimated in a manner analogous to that described above for the dissociation reactions (i.e., using the frequencies of **I** and removing one mode (508 cm^{-1}) for the reaction coordinate, $\Delta S^{\ddagger}(600\ K) = -7$ J K^{-1} mol^{-1}). In this reaction, the almost free internal rotation present in the equilibrium structure **I** will disappear in the transition state, and so the mode was included in the $\rho(E)$ calculation as a vibration. The unknown in this process is the activation energy. However, since the isomerization competes with the dissociation to CH_3CNH^+ and CH_3OH on the microsecond time scale (the MI spectrum), the E_0 for the isomerization can be adjusted to produce the desired overlapping log $k(E)$ vs E curves (Figure 3).

Although the ratio of $k_{(\mathbf{I}\rightarrow products)}$ to $k_{(\mathbf{I}\rightarrow\mathbf{II})}$ rigorously does not equal the relative product ion abundances,[28] the similar intensities of m/z 42 and m/z 56 in the MI mass spectrum means that this relationship will be approximately correct. Therefore, for reaction rate constants on the order of 10^5 s^{-1}, the log $k(E)$ vs E curve for the isomerization must be slightly lower than that for the simple dissociation to m/z 42. At longer time scales (and lower values of log $k(E)$), the isomerization competes more favorably (Table 1) and hence the curves should cross at ca. 5 × 10^4 s^{-1}.[29] This puts considerable constraint on E_0 for the isomerization, which was modeled to be 115 kJ mol^{-1}. Thus, it is likely that the transition state connecting **I** with **II**/**III** lies within 10 kJ mol^{-1} of this value. For comparison, Figure 3 shows the log $k(E)$ vs E curves obtained with E_0 values of 115 and 125 kJ mol^{-1}.

5. Summary

The final reaction surface that is obtained from the experimental and theoretical evidence is presented in Figure 4. The transition structure for isomerization of the proton-bound dimer lies 10 kJ mol^{-1} below the threshold for dissociation to protonated acetonitrile and methanol. At the internal energies probed in the MI experiments reported here, there is an isomer of the original proton-bound dimer that consists of a $CH_3CNCH_3^+$ backbone with a molecule of water migrating freely around it. The low binding energy of this isomer, 40 kJ mol^{-1}, accounts for our inability to generate it from other reactions (such as the reaction of CH_3CN, CH_3I, and H_2O) at the pressures obtainable

in our ion source. The theoretical binding energy of the proton-bound dimer, 121 kJ mol^{-1}, allows us to determine the absolute energies of other acetonitrile−methanol proton-bound cluster ions, based on their relative energies as measured by El-Shall et al.[9b]

Acknowledgment. P.M.M. thanks the Natural Sciences and Engineering Research Council of Canada for financial support and the University of Ottawa for a grant toward the purchase of a computer workstation. The author also thanks Dr. O. Mazyar (University of North Carolina at Chapel Hill) for assistance in developing the RRKM program, and the reviewer of this manuscript for valuable comments.

References and Notes

(1) For examples, see the following. (a) Kebarle, P. In *Techniques for the Study of Ion−Molecule Reactions*; Farrar, J. M., Saunders, W. H., Eds.; Wiley-Interscience: New York, 1988. (b) Meot-Ner, M. *J. Am. Chem. Soc.* **1984**, *106*, 1265. (c) Hiraoka, K.; Takimoto, H.; Yamabe, S. *J. Phys. Chem.* **1986**, *90*, 5910. (d) Castleman, A. W.; Wei, S. *Annu. Rev. Phys. Chem.* **1994**, *45*, 685. (e) Castleman, A. W.; Bowen, K. H. *J. Phys. Chem.* **1996**, *100*, 12911.

(2) Ferguson, E. E.; Fehsenfeld, F. C.; Albritton, D. L. In *Gas Phase Ion Chemistry*; Bowers, M. T., Ed.; Academic Press: New York, 1979.

(3) Yates, B. F.; Bouma, W. J.; Radom, L. *Tetrahedron* **1986**, *22*, 6225.

(4) For examples, see the following. (a) Harnish, D.; Holmes, J. L. *J. Am. Chem. Soc.* **1991**, *113*, 9729. (b) Morton, T. H. *Org. Mass Spectrom.* **1991**, *26*, 18.

(5) McAdoo, D. J.; Morton, T. H. *Acc. Chem. Res.* **1993**, *26*, 295 and references therein.

(6) For examples, see the following. (a) Schaftenaar, G.; Postma, R.; Ruttink, P. J. A.; Burgers, P. C.; McGibbon, G. A.; Terlouw, J. K. *Int. J. Mass Spectrom. Ion Processes* **1990**, *100*, 521. (b) Holmes, J. L.; Hop, C. E. C. A.; Terlouw, J. K. *Org. Mass Spectrom.* **1986**, *21*, 776. (c) Booze, J. A.; Baer, T. *J. Phys. Chem.* **1992**, *96*, 5715. (d) Mayer, P. M.; Baer, T. *J. Phys. Chem.* **1996**, *36*, 14949. (e) Mazyar, O. A.; Mayer, P. M.; Baer, T. *Int. J. Mass Spectrom. Ion Processes* **1997**, *167/168*, 389.

(7) For examples, see the following. (a) Szulejko, J. E.; McMahon, T. B. *Org. Mass Spectrom.* **1993**, *28*, 1009. (b) Aviyente, V.; Iraqi, M.; Peres, T.; Lifshitz, C. *J. Am. Soc. Mass Spectrom.* **1991**, *2*, 113. (c) Audier, H. E.; Monteiro, C.; Mourgues, P.; Robin, D. *Rapid Commun. Mass Spectrom.* **1989**, *3*, 84.

(8) (a) Beauchamp, J. L.; Caserio, M. C. *J. Am. Chem. Chem.* **1972**, *94*, 2638. (b) Beauchamp, J. L.; Caserio, M. C.; McMahon, T. B. *J. Am. Chem. Soc.* **1974**, *96*, 6243. (c) Mafune, F.; Kohno, J.; Kondow, T. *J. Phys. Chem.* **1996**, *100*, 10041. (d) Zhang, X.; Yang, X.; Castleman, A. W. *Chem. Phys. Lett.* **1991**, *185*, 298. (e) Feng, W. Y.; Iraqi, M.; Lifshitz, C. *J. Phys. Chem.* **1993**, *97*, 3510. (f) Feng, W. Y.; Lifshitz, C. *Int. J. Mass Spectrom. Ion Processes* **1995**, *149/150*, 13.

(9) (a) Deakyne, C. A.; Meot-Ner, M.; Campbell, C. L.; Huges, M. G.; Murphy, S. P. *J. Chem. Phys.* **1986**, *84*, 4958. (b) El-Shall, M. S.; Olafsdottir, S. R.; Meot-Ner, M.; Sieck, L. W. *Chem. Phys. Lett.* **1991**, *185*, 193. (c) Graul, S. T.; Squires, R. R. *Int. J. Mass Spectrom. Ion Processes* **1989**, *94*, 41. (d) Honma, K.; Sunderlin, L. S.; Armentout, P. B. *J. Chem. Phys.* **1993**, *99*, 1623. (e) Vinogradov, P. S.; Borisenko, D. M.; Lindinger, W.; Taucher, J.; Hansel, A. Proceedings of the 45th American Society for Mass Spectrometry Conference and Exhibition, Palm Springs, California, June 1−5, 1997. (f) Zhang, X.; Castleman, A. W. *Int. J. Mass Spectrom. Ion Processes* **1995**, *149/150*, 521.

(10) Holmes, J. L.; Mayer, P. M. *J. Phys. Chem.* **1995**, *99*, 1366.

(11) Busch, K. L.; Glish, G. L.; McLuckey, S. A. *Mass Spectrometry/Mass Spectrometry*; VCH Publishers: New York, 1988.

(12) Hehre, W. J.; Radom, L.; Schleyer, P. v. R.; Pople, J. A. *Ab Initio Molecular Orbital Theory*; Wiley: New York, 1986.

(13) Frisch, M. J.; Trucks, G. W.; Schlegel, H. B.; Gill, P. M. W.; Johnson, B. G.; Robb, M. A.; Cheesman, J. R.; Keith, T.; Petersson, A.; Montgomery, A.; Raghavachari, K.; Al-Laham, M. A.; Zakrzewski, V. G.; Ortiz, J. V.; Foresman, J. B.; Cioslowski, J.; Stefanov, B. B.; Nanayakkara, A.; Challacombe, M.; Peng, C. Y.; Ayala, P. Y.; Chen, W.; Wong, M. W.; Andres, A. L.; Replogle, E. S.; Gomperts, R.; Martin, R. L.; Fox, D. J.; Binkley, J. S.; Defrees, D. J.; Baker, J.; Stewart, J. P.; Head-Gordon, M.; Gonzalez, C.; Pople, J. A. *GAUSSIAN 94*, revision E.1; Gaussian, Inc.: Pittsburgh, 1995.

(14) Mayer, P. M. *J. Chem. Phys*., in press.

(15) Curtiss, L. A.; Raghavachari, K.; Trucks, G. W.; Pople, J. A. *J. Chem. Phys.* **1991**, *94*, 7221.

(16) Curtiss, L. A.; Raghavachari, K.; Pople, J. A. *J. Chem. Phys.* **1993**, *98*, 1293.

(17) Curtiss, L. A.; Redfern, P. C.; Smith, B. J.; Radom, L. *J. Chem. Phys.* **1996**, *104*, 5148.

(18) Curtiss, L. A.; Raghavachari, K.; Pople, J. A. *J. Chem. Phys.* **1995**, *103*, 4192.

(19) Nicolaides, A.; Rauk, A.; Glukhovtsev, M. N.; Radom, L. *J. Phys. Chem.* **1996**, *100*, 17460.

(20) Lias, S. G.; Bartmess, J. E.; Liebman, J. F.; Holmes, J. L.; Levin, R. D.; Mallard, W. G. *J. Phys. Chem. Ref. Data* **1988**, *17* (Suppl. 1).

(21) (a) McEwan, M. J.; Denison, A. B.; Huntress, W. T.; Anicich, V. G.; Snodgrass, J.; Bowers, M. T. *J. Phys. Chem.* **1989**, *93*, 4064. (b) Smith, S. C.; Wilson, P. F.; Sudkeaw, P.; MacIagan, R. G. A. R.; McEwan, M. J.; Anicich, V. G.; Huntree, W. T. *J. Chem. Phys.* **1993**, *98*, 1944. (c) Wilson, P. F.; Freeman, C. G.; McEwan, M. J. *Int. J. Mass Spectrom. Ion Processes* **1993**, *128*, 83.

(22) The competing formation of *m*/*z* 15 (CH_3^+) and *m*/*z* 18 (CD_3^+) in the He CID mass spectrum of $CD_3CNCH_3^+$ is consistent with the relative stabilities of the accompanying neutral products CH_3NC and CD_3CN.

(23) Hunter, E. P.; Lias, S. G. Proton Affinity Evaluation. In *NIST Chemistry WebBook, NIST Standard Reference Database Number 69*; Mallard, W. G., Linstrom, P. J., Eds.; National Institute of Standards and Technology: Gaithersburg, MD, 1988.

(24) Ruttink, P. J. A. *J. Phys. Chem.* **1987**, *91*, 703 and references therein.

(25) Daley, G. M.; Meot-Ner, M.; Pithawalla, Y. B.; El-Shall, M. S. *J. Chem. Phys.* **1996**, *104*, 7965.

(26) Baer, T.; Hase, W. L. *Unimolecular Reaction Dynamics, Theory and Experiments*; Oxford University Press: New York, 1996.

(27) Scott, A. P.; Radom, L. *J. Phys. Chem.* **1996**, *100*, 16502.

(28) Holmes, J. L.; Aubry, C. A.; Mayer, P. M. *J. Phys. Chem. A*, in press.

(29) The average *k* values for each FFR are dependent on the accelerating potential, instrument geometry, and ion mass. The values reported here represent the most probable *k*, but the distribution of *k* that can lead to observable fragmentation reactions extends over 2 orders of magnitude.[28]